

Original Article

Imbalance of a KLF4-miR-7 auto-regulatory feedback loop promotes prostate cancer cell growth by impairing microRNA processing

Lian-Zi Wei^{1*}, Yan-Qing Wang^{2*}, Yun-Li Chang¹, Na An¹, Xiao Wang¹, Pei-Jie Zhou¹, Helen He Zhu¹, Yu-Xiang Fang¹, Wei-Qiang Gao^{1,3,4}

¹State Key Laboratory of Oncogenes and Related Genes, Renji-Med X Clinical Stem Cell Research Center, Ren Ji Hospital, School of Medicine, Shanghai Jiao Tong University, Shanghai, China; ²Department of Urology, Ren Ji Hospital, School of Medicine, Shanghai Jiao Tong University, Shanghai, China; ³School of Biomedical Engineering & Med-X Research Institute, Shanghai Jiao Tong University, Shanghai, China; ⁴Collaborative Innovation Center of Systems Biomedicine, Shanghai Jiao Tong University, Shanghai, China. *Equal contributors.

Received October 30, 2017; Accepted November 14, 2017; Epub February 1, 2018; Published February 15, 2018

Abstract: The microRNA-transcription factor auto-regulatory feedback loop is a pivotal mechanism for homeostatic regulation of gene expression, and dysregulation of the feedback loop is tightly associated with tumorigenesis and progression. However, the mechanism underlying such dysregulation is still not well-understood. Here we reported that Krüppel-like factor 4 (KLF4), a stemness-associated transcription factor, promotes the transcription of miR-7 to repress its own translation so that a KLF4-miR-7 auto-regulatory feedback loop is established for mutual regulation of their expression. Interestingly, this feedback loop is unbalanced in prostate cancer (PCa) cell lines and patient samples due to an impaired miR-7-processing, leading to decreased mature miR-7 production and attenuated inhibition of KLF4 translation. Mechanistically, enhanced oncogenic Yes associated protein (YAP) nuclear translocation mediates sequestration of p72, a co-factor of the Drosha/DGCR8 complex for pri-miR-7s processing, leading to attenuation of microprocessors' efficiency. Knockdown of YAP or transfection with a mature miR-7 mimic can significantly recover miR-7 expression to restore this feedback loop, and in turn to inhibit cancer cell growth by repressing KLF4 expression *in vitro*. Thus, our findings indicate that targeting the KLF4-miR-7 feedback loop might be a potential strategy for PCa therapy.

Keywords: KLF4, microRNA processing, miR-7, prostate cancer, YAP

Introduction

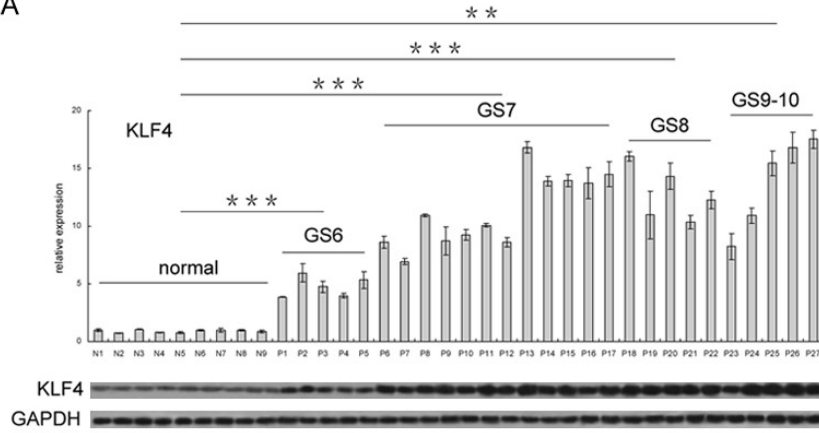
MicroRNAs (miRNAs) are a class of small non-coding RNAs that post-transcriptionally regulate mRNA stability and translation of target mRNAs by recognizing and binding with the mRNA 3'UTR region [1]. It is well known that miRNAs are involved in pathogenesis of various types of human cancers and have a crucial oncogenic or tumor suppressive function in cancer progression [2]. For example, microRNA-7 (miR-7) has recently been found to be down-regulated and to play a tumor suppressor role in several kinds of cancers by targeting different oncogenes and pro-tumorigenic pathways [3]. Fang Y et al. demonstrated that miR-7 arrests cell cycles in G0/G1 phase and inhibits tumor proliferation by targeting PIK3-

CD, a key catalytic subunit of PI3K in tumors, and the PI3K/Akt/mTOR pathway in hepatocellular carcinoma (HCC) [4]. In additions, miR-7 can also inhibit 1) breast cancer growth by targeting p21-activated kinase 1 (PAK1) [5], 2) epithelial-to-mesenchymal transition (EMT) of breast cancer stem-like cells by targeting SET domain bifurcated 1 (SETDB1) and STAT3 pathway [6], 3) brain metastasis of breast cancer stem-like cells by regulating the expression of Krüppel-like factor 4 (KLF4) [7]. In our previous work, we also demonstrated that miR-7 inhibits the stemness of prostate cancer (PCa) stem-like cells and tumorigenesis by targeting KLF4 and repressing the KLF4/PI3K/Akt/p21 pathway [8].

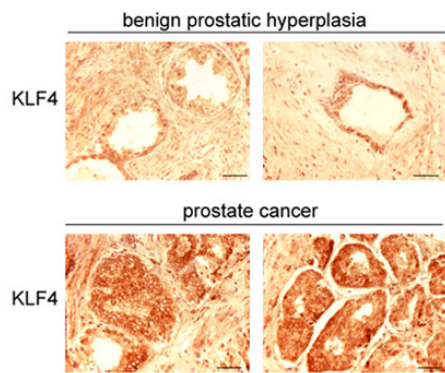
As a pivotal stemness-associated transcription factor, KLF4 is a *bona fide* target of miR-7 and

Imbalance of a KLF4-miR-7 loop promotes prostate cancer cell growth

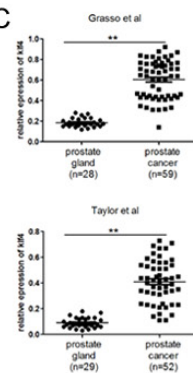
A



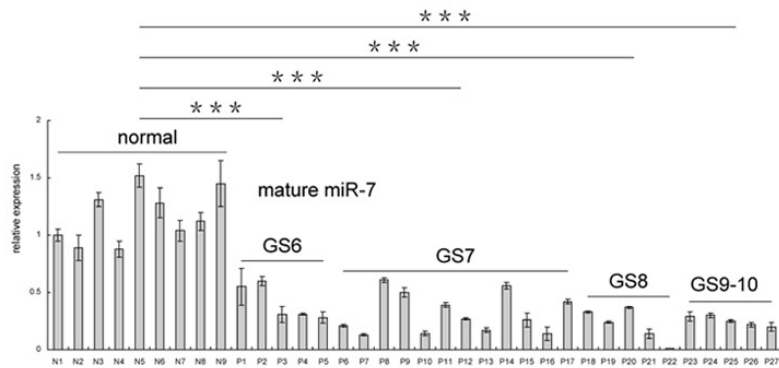
B



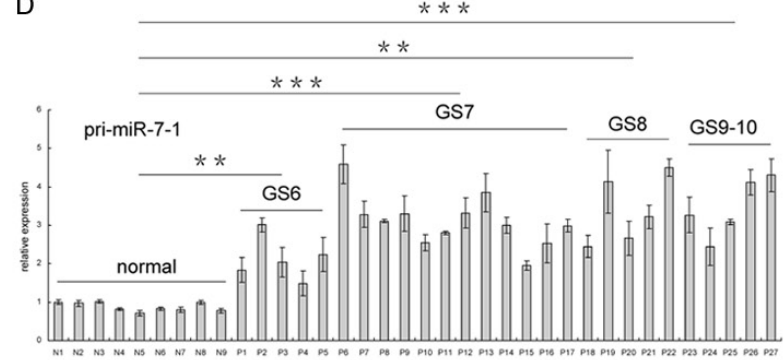
C



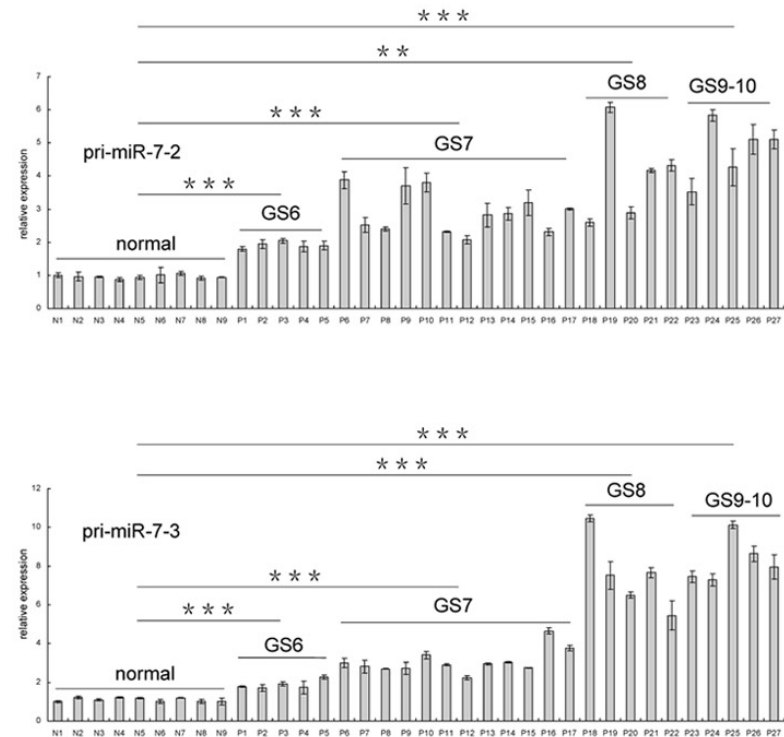
E



D



E



Imbalance of a KLF4-miR-7 loop promotes prostate cancer cell growth

Figure 1. Expression of KLF4 and pri-miR-7s is upregulated but that of mature miR-7 is downregulated in clinical patient samples. A. Expression of KLF4 in both patient tumor samples (P1 to P27) and BPH samples (N1 to N9) is measured by qRT-PCR and western blot. B. Expression of KLF4 is upregulated in PCa samples by IHC staining. C. Data from two independent datasets in Oncomine database demonstrates a significant upregulation of KLF4 expression in PCa tissues compared to normal controls. D. Transcription of pri-miR-7s is significantly upregulated in patient tumor samples. E. Expression of mature miR-7 is downregulated in PCa samples. Scale Bar: 50 μ m; ***: $P < 0.001$; **: $P < 0.01$.

activates or represses the transcription of multiple genes including microRNAs and is involved in regulation of tumorigenesis and progression [9]. It has been reported that KLF4 inhibits liver cancer cell growth and invasion by activating the transcription of miR-153, miR-506 and miR-200b, which in turn reduces expression of EMT-related proteins Snail1, Slug and Zeb1 [10]. In addition, in breast cancer cells KLF4 induces miR-206 expression to repress its own translation, forming a negative feedback loop to inhibit tumor growth, invasion and migration [11]. Such transcription factor-microRNA auto-regulatory feedback loops (i.e. Zeb1-miR-200 feedback loop) have been also identified to be associated with promotion of tumorigenicity and stemness-maintenance of cancer stem cells [12-14]. However, how KLF4 regulates the transcription of miR-7 in PCa and whether a miR-7-KLF4 auto-regulatory feedback loop can be formed to promote or repress proliferation of PCa cells is unknown.

In the present study, we demonstrated for the first time that KLF4 activates the transcription of miR-7 in PCa cells to reversely suppress its own translation. The KLF4-miR-7 auto-regulatory feedback loop contributes to the regulation of both KLF4 and miR-7 expression, but is unbalanced in PCa caused by an impaired p72-dependent microRNA-processing.

Material and methods

Plasmids

KLF4 shRNA (TG316853) expression vector and control vector (TR30013) were purchased from Origene (Rockville, MD, USA). A firefly luciferase expressional vector pHEW-luc [8] was employed as backbone for dual-luciferase report assay. Truncated promoter fragments of pri-miR-7-1, pri-miR-7-2 and pri-miR-7-3 (shown in **Figure 3**) were amplified from genomic DNA by PCR using specific primers (**Table 1**) and sequentially double digested with PacI and BglII (New England Biolabs, Ipswich, MA, USA) for

inserting to the backbone vector, which was double digested with PacI and BamHI (New England Biolabs), to replace the intrinsic EF1 α promoter for driving luciferase expression. All the constructions were confirmed by PCR and sequencing and then purified using Endotoxin-free Plasmid Extraction Kit (Qiagen, German) for transfection.

Cell culture and transfection

Human benign prostatic hyperplasia cell line BPH-1 and human prostate cancer cell lines PC3 and LNCaP were purchased from ATCC (Manassas, VA, USA). All cell lines used were cultured in RPMI 1640 basic medium with 10% FBS (Thermo Fisher Scientific, Waltham, MA, USA) and maintained at 37°C and 5% CO₂. Transfection was performed with Lipofectamine 3000 (Thermo Fisher Scientific). Puromycin (Sigma-Aldrich, St. Louis, MO, USA) was used for selecting subclones stably expressing KLF4-shRNA or scrambled control shRNA. For luciferase assay, 2 $\times 10^5$ cells per well in 24-well plate were co-transfected with 500 ng variant truncated promoter driven luciferase expression vector and 5 ng Renilla luciferase expression vector (internal control). YAP siRNA, p72 siRNA or scrambled siRNA control (final concentration: 50 μ M) and 20 μ M miR-7 mimic or scrambled mimic control (Thermo Fisher Scientific) were transfected with Lipofectamine RNAiMax (Thermo Fisher Scientific) respectively.

RNA extraction and qRT-PCR

Total RNAs were isolated from cell lines and tissue samples using Trizol (Thermo Fisher Scientific), and the protocol was previously described [8]. MiRNA was extracted using miRNA isolation kit (Thermo Fisher Scientific) according to the manufacturers' instruction. MiRNA reverse transcription and qRT-PCR were carried out using Taqman miRNA reverse transcription kit (Thermo Fisher Scientific) and Taqman premix (Takara, Shiga, Japan) respec-

Imbalance of a KLF4-miR-7 loop promotes prostate cancer cell growth

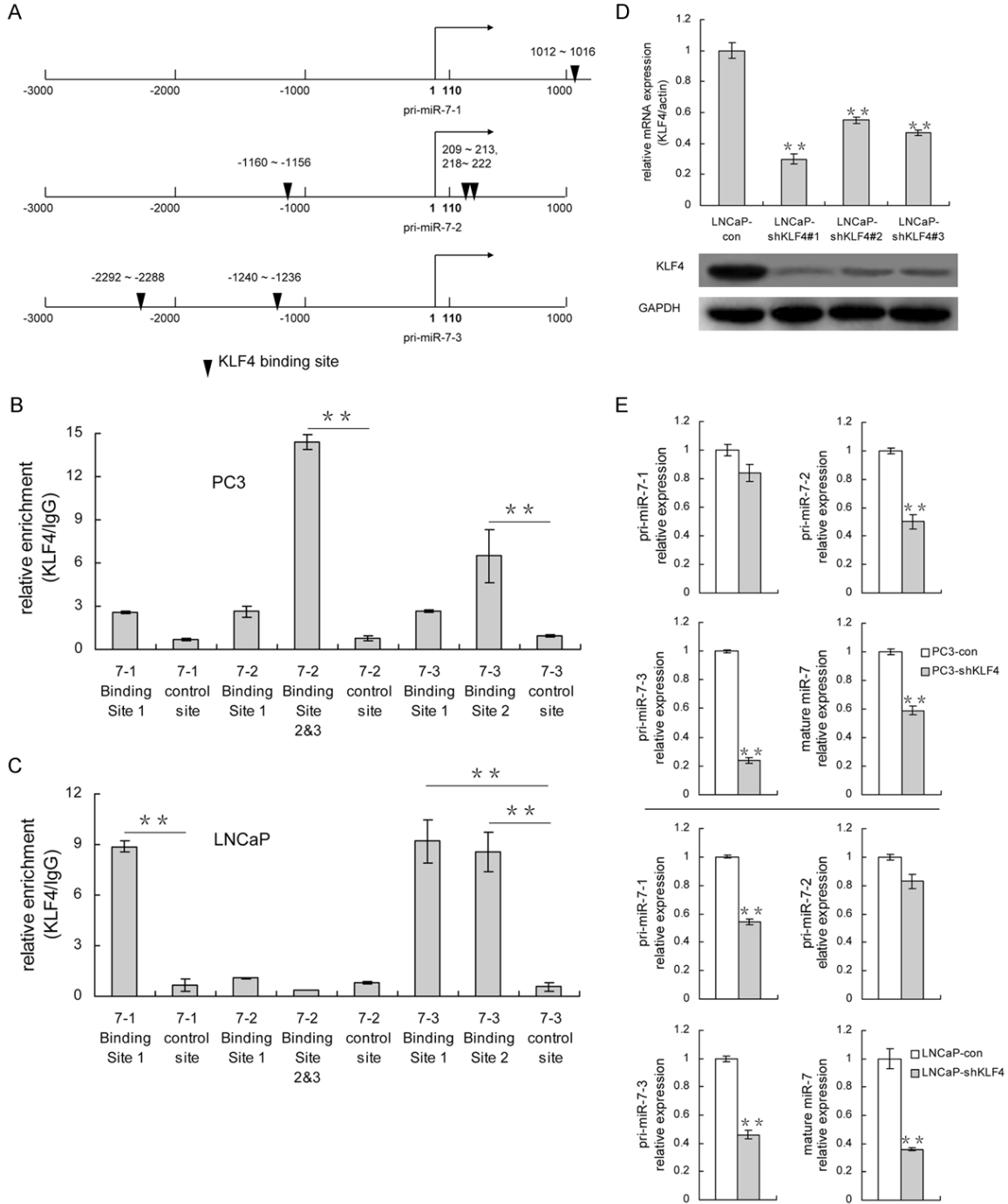


Figure 2. KLF4 activates the transcription of three miR-7 primary precursors in both PC3 and LNCaP cells. (A) Schematic of predicted KLF4 binding sites on promoter regions of three miR-7 primary precursors. (B, C) Relative enrichment of KLF4 at its binding sites was measured by ChIP assay in PC3 (B) and LNCaP (C) cells. (D) Expression of KLF4 can be inhibited by three independent KLF4 shRNA expressional vectors. The vector expressing shKLF4#1 is selected for construction of KLF4 stable knockdown subclone cell line in LNCaP cells for subsequent experiments due to its best effect on inhibition of KLF4 expression. (E) Knockdown of KLF4 represses expression of both miR-7 primary precursors and mature miR-7 in PC3 and LNCaP cells. **: P<0.01.

tively. The specific reverse primers and qRT-PCR Taqman probes for miR-7 and snRNA U44

(internal normalization control) were purchased from Thermo Fisher Scientific. For mRNA

Imbalance of a KLF4-miR-7 loop promotes prostate cancer cell growth

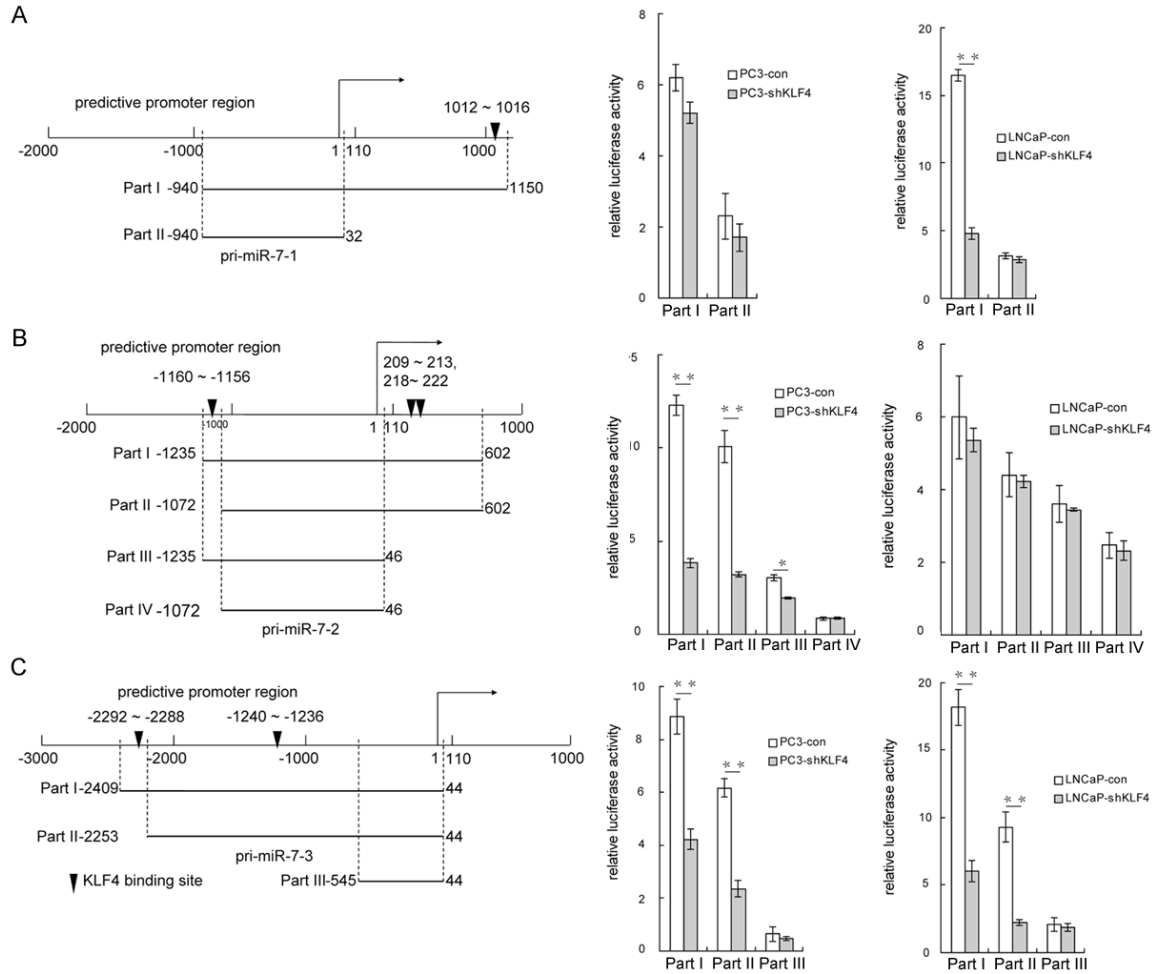


Figure 3. KLF4 activates downstream transcription in PC3 and LNCaP cells. (A-C) Regulation of KLF4 on the transcription of miR-7 primary precursors is evaluated by dual-luciferase report assay in PC3 and LNCaP cells. Truncated promoters of pri-miR-7-1 (A), pri-miR-7-2 (B) and pri-miR-7-3 (C) with or without KLF4 binding sites are used to drive luciferase expression in PC3-shKLF4 vs. PC3-con and LNCaP-shKLF4 vs. LNCaP-con cells respectively. **: $P < 0.01$; *: $P < 0.05$.

analysis, cDNAs were synthesized from 1 μ g total RNA with Prime-Script RT kit (Takara) and amplified with SYBR Green Real-time PCR Master Mix (Thermo Fisher Scientific). All primers for mRNA expression assay are available in **Table 2**.

Western blot and co-immunoprecipitation (co-IP)

The total proteins and the nucleus proteins were obtained from cell lines and tissue samples using RIPA buffer (Beyotime Inst Biotech, Haimen, Jiangsu, China) and Nuclear Extract Kit (Thermo Fisher Scientific) respectively. For co-IP, nucleus lysates were treated with Protein A/G Sepharose beads (Sigma-Aldrich) and

incubated with p72 antibodies or IgG (Santa Cruz Biotechnology, Dallas, TX, USA) at 4°C overnight. Beads were washed 3 times with PBS and sequentially the loading buffer was added and incubated at 95°C for 5 mins. After centrifugation at 20,000 g for 1 min, the supernatants were collected for western blot analysis using relevant primary antibodies (shown in **Table 3**). Total protein extractions and nucleus lysates were separated by SDS-PAGE, followed by the transfer onto nitrocellulose membranes. The membranes were blocked and probed with primary and secondary antibodies sequentially. Specific proteins were detected with Immobilon Western Chemiluminescent HRP Substrate (Millipore, Bedford, MA, USA).

Imbalance of a KLF4-miR-7 loop promotes prostate cancer cell growth

Table 1. Primers for amplification of truncated promoter fragments from genomic DNA

Name	Primer	Sequence (5' to 3')		
Pri-miR-7-1	Part I	Forward	CGCTTAATTA ^a GGCTCATATGGTGATCTTGG	
		Reverse	CCCAGATCT ^b CAGCAATAGACTTCCAAACC	
	Part II	Forward	CGCTTAATTAAGGCTCATATGGTGATCTTGG	
		Reverse	CCCAGATCTTAGTCTTCCACACAGAACTAG	
Pri-miR-7-2	Part I	Forward	GCGTTAATTAAGGTATTGCCAGTCTTCTCC	
		Reverse	TCCAGATCTATACACACAAGTCCACTCCC	
	Part II	Forward	CCGTTAATTAAGCAGCACCAATAGGGAAG	
		Reverse	TCCAGATCTATACACACAAGTCCACTCCC	
	Part III	Forward	GCGTTAATTAAGGTATTGCCAGTCTTCTCC	
		Reverse	CAGAGATCTTCACTAGTCTTCCAGATGGG	
	Part IV	Forward	CCGTTAATTAAGCAGCACCAATAGGGAAG	
		Reverse	CAGAGATCTTCACTAGTCTTCCAGATGGG	
	Pri-miR-7-3	Part I	Forward	CCATTAATTAACCTCCCAAAGTGCTCAGATT
			Reverse	TCCAGATCTTCACTAGTCTTCCACACAGC
		Part II	Forward	CCCTTAATTAACATGCAATCCACACCATATC
			Reverse	TCCAGATCTTCACTAGTCTTCCACACAGC
Part III		Forward	CCCTTAATTAACCTCTTGACCTCTTCATCCG	
		Reverse	TCCAGATCTTCACTAGTCTTCCACACAGC	

a: Underlined "TTAATTA" fragment is the recognition site for *PacI* digestion. b: Underlined "AGATCT" fragment is the recognition site for *BglII* digestion.

Table 2. Primers for qRT-PCR

Name	Primer	Sequence (5' to 3')
KLF4	Forward	TTACCAAGAGCTCATGCCAC
	Reverse	TGTGCCTTGAGATGGGAACT
p72	Forward	AGCAGTTTAGTGGGATAGGC
	Reverse	AGGGTATTGGTAGGCAGTCT
Drosha	Forward	GGACCAAGTATTCAGCAAGC
	Reverse	GCTCTCTTCCACCTCATT
DGCR8	Forward	AGTGTGATTGAGCTGCAGCA
	Reverse	CTTGGGCTTCTTTCGAGTCT
Dicer	Forward	AAGGTCAGAGTCACTGTGGA
	Reverse	CCTGAGGTTGATTAGCTTTG
YAP	Forward	ATGTGGACCTTGGAACACTG
	Reverse	GCAGCCAAAACAGACTCCAT
pri-miR-7-1	Forward	GGTGA ^a AACTGCTGCCAAAAC
	Reverse	GCTAGTAAGGTGTGAAATGCTG
pri-miR-7-2	Forward	CTGAAGGAGCATCCAGACCG
	Reverse	GAACACGTGGAAGGATAGCC
pri-miR-7-3	Forward	TCAGGTGAGAAGGAGGAGCTG
	Reverse	TGTATCGCCTGGAGTGAGCC

Dual-luciferase reporter assay

Forty-eight hours after transfection, luciferase activities were measured with the Dual-

Luciferase Reporter Assay System (Promega, Madison, WI, USA). Reporter luciferase activity was normalized to the internal control Renilla luciferase activity in all samples.

Cell proliferation assay

Cell proliferation was measured by Cell Counting Kit-8 (CCK-8) (Beyotime Inst Biotech) according to the manufacturer's protocols. Briefly, 3×10^3 cells per well were seeded into 96-well plates for standard culture. Subsequently, 10 μ l of CCK-8 reagent was added to each well at 0, 24, 48, 72, and 96 h after inoculation respectively, followed by continuous incubation at 37°C for 2 hrs. Finally, the absorbance values were measured at 450 nm using BioTek Synergy HT microplate reader. Measurement was performed for five wells as repeat at each

time point and the experiment was repeated for three times.

2D-colony formation assay

One week after seeding cells in 6-well plate for standard culture, formed colonies were stained with 0.1% crystal violet (Sigma-Aldrich) for imaging and counting.

3D-sphere formation assay

Five hundred cells per well were coated with solidified mixture (1:1) of geltrex (Thermo Fisher Scientific) and matrigel (BD Biosciences, San Jose, CA, USA) and seeded in 24-well plate for standard culture. Two weeks after inoculation, spheres were imaged and counted in 10 random fields.

Chromatin immunoprecipitation (ChIP)

The CHIP assay kit (#9003) was purchased from Cell Signaling Technology (Danvers, MA, USA) and the experiment was performed by following the protocol. To examine the changes of KLF4 enrichment on the promoter regions of three miR-7 primary precursors respectively,

Imbalance of a KLF4-miR-7 loop promotes prostate cancer cell growth

Table 3. Primary antibodies used in the study

Antibody	Company	Catalog Number
KLF4	Santa Cruz Biotechnology	sc-20691
p72	Santa Cruz Biotechnology	sc-376396
AR	Cell Signaling Technology	#3202
YAP	Cell Signaling Technology	#4912
Drosha	Cell Signaling Technology	#3364
DGCR8	Cell Signaling Technology	#6914
GAPDH	Cell Signaling Technology	#2118
Dicer	Proteintech	20567-1-AP
TBP	Proteintech	66166-1-Ig

Table 4. Primers for CHIP assay

Name	Primer	Sequence (5' to 3')	
Pri-miR-7-1 Binding site 1	Forward	GCTGAATTTCCCAACCCAC	
	Reverse	CTTCCAGCAATAGACTTCC	
	Control site	Forward	AGGTGGTCAGCGGATTAAC
		Reverse	GTGCATTCTGTATCTGGTCC
Pri-miR-7-2 Binding site 1	Forward	ACTCAGAGCTAGGTATTGCC	
	Reverse	TGAGCACTTCTCTTTAGCC	
	Binding site 2&3	Forward	GTTGTTGTCTTACTGCGCTC
		Reverse	TGTTTCTGGAAGAGTCTGCC
	Control site	Forward	AAGCGTTGCTAAGGGAACAG
		Reverse	AATTGGGAGAAGATGCAAGC
Pri-miR-7-3 Binding site 1	Forward	AAGTTTTGCACCTGAGGCTG	
	Reverse	TTTGGGACATTGGGCACAGT	
	Binding site 2	Forward	TATCAGTGCTAGTTGCGACC
		Reverse	CCCTCGTGCTGAAGAAAAC
	Control site	Forward	GTGAAGCTGTAAGTCAACCC
		Reverse	TGCCTCCCTGTTTTCCATTC

ChIP assays were performed using anti-KLF4 antibody (Santa Cruz Biotechnology) as protocol described. After extraction of ChIP DNA, specific fragments (less than 200 bp) containing potential binding sites or control sites (more than 1 kb faraway from potential KLF4 binding sites and without core recognition sequence of KLF4) were amplified and analyzed by qPCR and sequencing. KLF4 relative enrichment was calculated by the formula provided in the protocol. Primers used for ChIP assay are available in **Table 4**.

Immunohistochemical (IHC) staining and microscopy

Tissues were fixed with 4% paraformaldehyde for 24 hrs and embedded in paraffin. Paraffin sections were dewaxed in xylene for 5 mins, consequentially hydrated in 100%, 95%, 85%

and 70% ethanol for 3 mins each, respectively, and rinsed three times in water. Sections were treated with disodium-hydrogen phosphate-2-hydrate for 15 mins to inactivate endogenous peroxidase and then blocked with 10% normal goat serum for 1 h at room temperature for IHC staining. After serum blocking, sections were incubated with KLF4 or YAP antibody (1:200, diluted in PBS with 1% normal goat serum) overnight at 4°C. Sections were washed with PBS for three times (10 mins each) and then incubated with horseradish peroxidase conjugated secondary antibody (Vector, Burlingame, CA, USA) for 1 h at room temperature. Sections were washed with PBS for three times again before DAB staining (Sangon Biotech, Shanghai, China) and hematoxylin counterstaining (Beyotime Inst Biotech). IHC staining was visualized under a microscope (Leica DFC420C) and images were merged using the ImageJ software.

Clinical samples

Frozen prostatic tumor mass (n=27 for qRT-PCR and western blot, n=2 for IHC) and benign prostatic hyperplasia (BPH) tissue mass (n=9 for qRT-PCR and western blot, n=2 for IHC) were obtained from the Ren Ji Biobank, Ren Ji Hospital, Shanghai Jiao Tong

University School of medicine [15]. Written informed consent was obtained from all patients. The studies using human tissues conformed to the provisions of the Declaration of Helsinki and were reviewed and approved by the Committee for Ethical Review of Research Involving Human Subjects at Ren Ji Hospital. Total RNAs, miRNAs and proteins were extracted from samples respectively under the same condition as described above. KLF4 and YAP expression was detected by qRT-PCR, western blot and IHC. Expression of miR-7 primary precursors and mature miR-7 was detected by qRT-PCR.

Statistical analysis

Independent two-sided Student's *t*-test and analysis of variance (ANOVA) were used for comparisons of differences between two gr-

Imbalance of a KLF4-miR-7 loop promotes prostate cancer cell growth

Table 5. Clinical data for 9 benign prostatic hyperplasia (BPH) tissue controls and 27 patient tumor tissues for qRT-PCR, western blot and co-IP assay

	Age	Gleason Score	TNM stage	PSA (ng/ml)
N1 ^a	66	- ^b	-	11.12
N2	76	-	-	14.44
N3	68	-	-	5.04
N4	66	-	-	1.31
N5	80	-	-	13.12
N6	78	-	-	13.09
N7	62	-	-	1.5
N8	77	-	-	9.57
N9	62	-	-	12.29
P1 ^c	69	6	T2bNOMO	16.99
P2	81	6	T2cNOMO	10.4
P3	69	6	T2bNOMO	7.1
P4	74	6	T2cNOMO	14
P5	69	6	T2cNOMO	9.576
P6	64	7	T2cNOMO	7.51
P7	64	7	T2cNOMO	24.56
P8	66	7	T3aNOMO	16.62
P9	80	7	T3bNOMO	51.14
P10	76	7	T2cN1MO	81.59
P11	64	7	T2bNOMO	16.66
P12	66	7	T2cNOMO	12
P13	71	7	T2cNOMO	15.56
P14	66	7	T2bNOMO	31.72
P15	66	7	T2cNOMO	12.62
P16	56	7	T2cNOMO	8
P17	63	7	T2cNOMO	5.81
P18	57	8	T2bNOMO	15.11
P19	72	8	T2bNOMO	9.2
P20	75	8	T3bNOMO	>200
P21	73	8	T2cNOMO	25.9
P22	68	8	T2cNOMO	33.35
P23	71	9	T3bNOMO	60.4
P24	75	10	T2bNOMO	6.52
P25	59	9	T2cNOMO	9.92
P26	67	9	T3bNOMO	22.97
P27	71	9	T2cNOMO	17.644

a: N1~N9: benign prostatic hyperplasia (BPH) tissues as normal controls. b: data not included. c: P1~P27: patient tumor tissues.

oups. All data were represented as mean \pm SEM from triplicate experiments. All the experiments were repeated for three times. Results were considered statistically significant when $P < 0.05$.

Results

Expression of KLF4 and three miR-7 primary precursors was upregulated but expression of mature miR-7 was downregulated in PCa clinical samples

In our previous work we found that KLF4 was upregulated in 90% clinical tumor samples and mature miR-7 was downregulated in 65% clinical tumor samples, indicating a negative relation between KLF4 and mature miR-7 expression [8]. In the present study we repeated to investigate expression of KLF4 and mature miR-7 in PCa clinical samples. Furthermore, we also investigated expression of three miR-7 primary precursors, which are named as pri-miR-7-1 (located at Chromosome 9), pri-miR-7-2 (located at Chromosome 15) and pri-miR-7-3 (located at Chromosome 19), respectively (**Figure 1**). We compared KLF4 expression in 27 tumor samples with variant Gleason Score (GS) to that in 9 BPH samples as normal control (**Table 5**). We found that consistent with our previous finding [8], KLF4 expression was significantly upregulated in tumor samples regardless of its GS (**Figure 1A**). By IHC staining, upregulation of KLF4 was again confirmed in tumor samples (**Figure 1B**; **Table 6**). In addition, data from Oncomine database (www.oncomine.org) also revealed an upregulation of KLF4 in PCa (**Figure 1C**). Notably, all of three miR-7 primary precursors were also overexpressed in relevant tumor samples (**Figure 1D**). In contrast, expression of mature miR-7 was significantly repressed in tumor samples (**Figure 1E**). Collectively, these results indicate that activated transcription of miR-7 primary precursors is associated with elevated expression of KLF in PCa and that attenuation on mature miR-7 production is involved in downregulation of mature miR-7 expression.

KLF4 activates the transcription of three miR-7 primary precursors in PCa cells

In order to explore whether and how KLF4 regulates the transcription of miR-7, we first predicated potential binding sites of KLF4 in promoter regions of three miR-7 primary precursors (**Figure 2A**) respectively via a bioinformatics assay (PROMO soft, <http://algggen.lsi.upc.es>). As shown in **Figure 2A**, there is one binding site in the promoter region of pri-miR-7-1, three binding sites in that of pri-miR-

Imbalance of a KLF4-miR-7 loop promotes prostate cancer cell growth

Table 6. Clinical data for 2 benign prostatic hyperplasia (BPH) tissue controls and 2 patient tumor tissues for IHC staining of KLF4 and YAP

	Age	Gleason Score	TNM stage	PSA (ng/ml)
BPH1 ^a	67	- ^b	-	9.31
BPH2	69	-	-	11.6
PCa1 ^c	73	8	T2cN1M0	97.2
PCa2	68	9	T3bN0M0	28.7

a: BPH1~BPH2: benign prostatic hyperplasia (BPH) tissues as normal controls. b: data not included. c: PCa1~PCa2: patient tumor tissues.

7-2 and two binding sites in that of pri-miR-7-3 respectively. We then investigated the enrichment of KLF4 at its potential binding sites by a ChIP assay in both AR-negative PCa cell line PC3 cells and AR-positive PCa cell line LNCaP cells. In PC3 cells, we found that KLF4 was enriched mainly at the binding site 2&3 in the promoter region of pri-miR-7-2 and secondarily at the binding site 2 in that of pri-miR-7-3 (**Figure 2B**). We repeated ChIP assays in LNCaP cells to confirm whether the enrichment pattern was similar to that in PC3 cells. Unexpectedly, in LNCaP cells KLF4 appeared to be enriched at all of the binding sites in the promoter region of pri-miR-7-1 and pri-miR-7-3 but not pri-miR-7-2, representing a different enrichment pattern from that in PC3 cells (**Figure 2C**).

Given that KLF4 can bind to the promoter regions of miR-7 primary precursors, we further investigated how KLF4 regulated miR-7 transcription in PCa cells. We first measured expression of three miR-7 primary precursors and mature miR-7 in a KLF4 knockdown PC3 subclone cell line (named PC3-shKLF4 with PC3-con as a control), which was established in our previous work [8], as well as a KLF4 knockdown LNCaP subclone cell line established in this study (**Figure 2D**). As shown in **Figure 2E**, KLF4 knockdown significantly inhibited the transcription of all the three miR-7 primary precursors and downregulated expression of mature miR-7 in both two cell lines. In order to further confirm these findings, we then constructed a series of truncated promoter-driven luciferase reporter vectors containing related binding sites for luciferase reporter assays (**Figure 3**). All vectors were transfected

into PC3-shKLF4 vs. PC3-con cells and LNCaP-shKLF4 vs. LNCaP-con cells respectively and the relative luciferase activity was measured 48 hrs after transfection. As shown in **Figure 3**, relative luciferase activity was significantly repressed as a response to KLF4 knockdown in PC3-shKLF4 when luciferase expression was driven by truncated promoters of pri-miR-7-2 and pri-miR-7-3 containing KLF4 binding site(s) but not that of pri-miR-7-1, consistent with the enrichment of KLF4 on relevant promoters in PC3 cells (**Figure 3A-C**). In LNCaP-shKLF4 cells, relative luciferase activity was also significantly repressed when luciferase expression was driven by truncated promoters of pri-miR-7-1 and pri-miR-7-3 containing KLF4 binding site(s) but not that of pri-miR-7-2 (**Figure 3A-C**). Taken together, these findings indicate that KLF4 can activate the transcription of three miR-7 primary precursors in both AR-negative and AR-positive PCa cells.

KLF4-miR-7 auto-regulatory feedback loop is unbalanced due to a decrease of mature miR-7 production through an impaired p72-dependent pri-miR-7s processing

Considering the above-described data together with our previous finding that miR-7 inhibits KLF4 expression at post-transcriptional level in PCa [8], we hypothesized that a KLF4-miR-7 auto-regulatory feedback loop can be formed for mutual regulation of KLF4 and miR-7 expression. However, results obtained from clinical tumor samples above revealed that expression of both KLF4 and miR-7 primary precursors was upregulated but that of mature miR-7 was downregulated (**Figure 1**). Based on that finding, we speculated that an imbalance occurred in this feedback loop and might be caused by an impaired microRNA processing, leading to a decrease of mature miR-7 production. Again we compared expression of miR-7 primary precursors and mature miR-7 in LNCaP and PC3 cells to that in human BPH cell line BPH-1. As expected, expression of three miR-7 primary precursors was significantly increased but that of mature miR-7 was significantly decreased in the PCa cells compared to that in the BPH-1 cell (**Figure 4A, 4B**). These data together demonstrate that overexpression of miR-7 primary precursors fails to increase the production of mature miR-7 to reversely inhibit KLF4 expression in PCa cells, which leads to an

Imbalance of a KLF4-miR-7 loop promotes prostate cancer cell growth

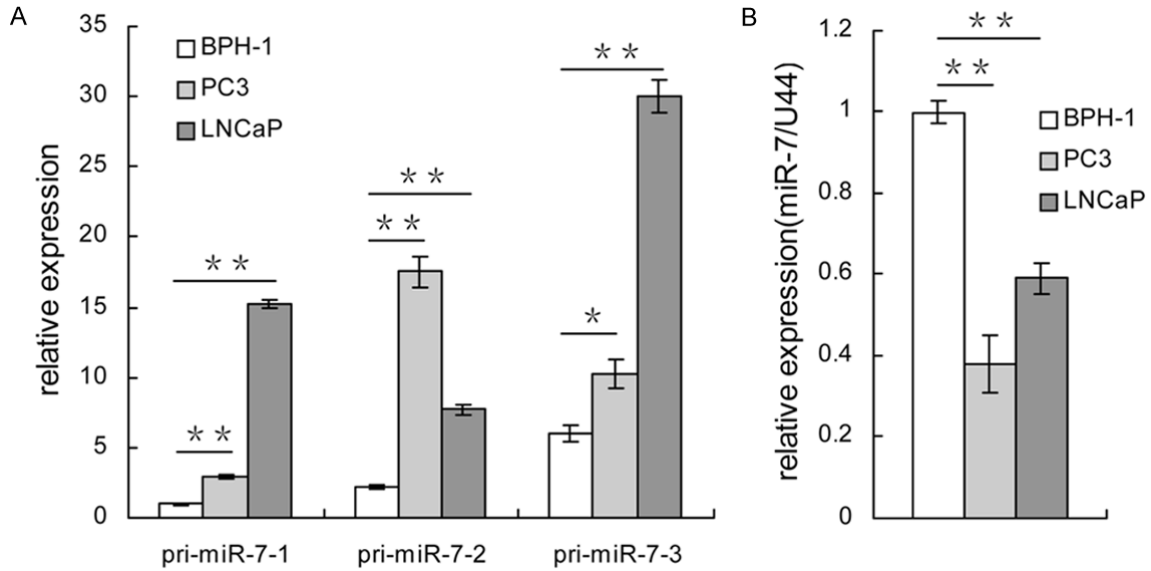


Figure 4. Upregulated transcription of miR-7 primary precursors fails to increase mature miR-7 production. A. Relative expression of pri-miR-7-1, pri-miR-7-2 and pri-miR-7-3 is quantified by qRT-PCR. B. Endogenous expression of mature miR-7 is quantified by TaqMan microRNA assay. **: P<0.01; *: P<0.05.

imbalance of the KLF4-miR-7 feedback loop. These findings also implicate that impaired or mutant pri-microRNA processing function may contribute to the decrease in mature miR-7 production.

It was previously reported that increased nuclear translocation of oncogenic YAP binds and sequesters p72, a co-factor of canonical pri-microRNA processing Drosha/DGCR8 complex [16], resulting in an attenuated efficiency for p72-dependent processing of pri-microRNAs to pre-microRNAs in cancer cells [17]. Interestingly, we found that there is one p72 binding site contained in the pri-miR-7-1 and pri-miR-7-3 respectively and four in the pri-miR-7-2, indicating that p72 might be involved in the processing of pri-miR-7-1, pri-miR-7-2 and pri-miR-7-3 to produce pre-miR-7 (Figure 5A). In order to investigate the relationship between p72 expression and mature miR-7 production, we downregulated p72 expression in PC3 and LNCaP cells as well as in BPH-1 cell and measured mature miR-7 expression (Figure 5B). We found that p72 knockdown significantly repressed expression of mature miR-7 especially in PC3 and LNCaP cells, indicating that the processing of miR-7 primary precursors is p72 dependent (Figure 5C). In addition, we compared endogenous expression of YAP, p72 and microprocessor complex components Dro-

sha and DGCR8 in PC3, LNCaP and BPH-1 cells. As shown in Figure 5D, all of these genes were overexpressed in PCa cell lines, especially in LNCaP cells compared to control BPH-1 cells, indicating that decreased production of mature miR-7 in PCa cells is not caused by downregulated expression of p72, Drosha or DGCR8. Furthermore, we confirmed that nuclear translocation of YAP was significantly increased in multiple PCa cell lines including PC3 and LNCaP (Figure 5E). Based on these findings, we herein hypothesized that enforced nuclear translocation of YAP disrupts the interaction of p72 with the Drosha/DGCR8 microprocessor complex via competitively binding to p72 and thus weakens p72-dependent miR-7 primary precursors processing. To confirm this hypothesis, we carried out co-IP assays to determine the interaction of p72 with YAP, Drosha and DGCR8 respectively. We found that the interaction between p72 and YAP was significantly enhanced in PCa cells. In contrast, the interaction of p72 with either Drosha or DGCR8 was weakened (Figure 5F). Consistent with observations in PCa cell lines, we found that the nuclear translocation of YAP was dramatically enhanced in clinical tumor samples (Figure 6A, 6B; Tables 5, 6). Furthermore, we repeated co-IP assay in one of the tumor samples (P23, with highest YAP expression) vs. one of the control samples (N4) to validate the interaction

Imbalance of a KLF4-miR-7 loop promotes prostate cancer cell growth

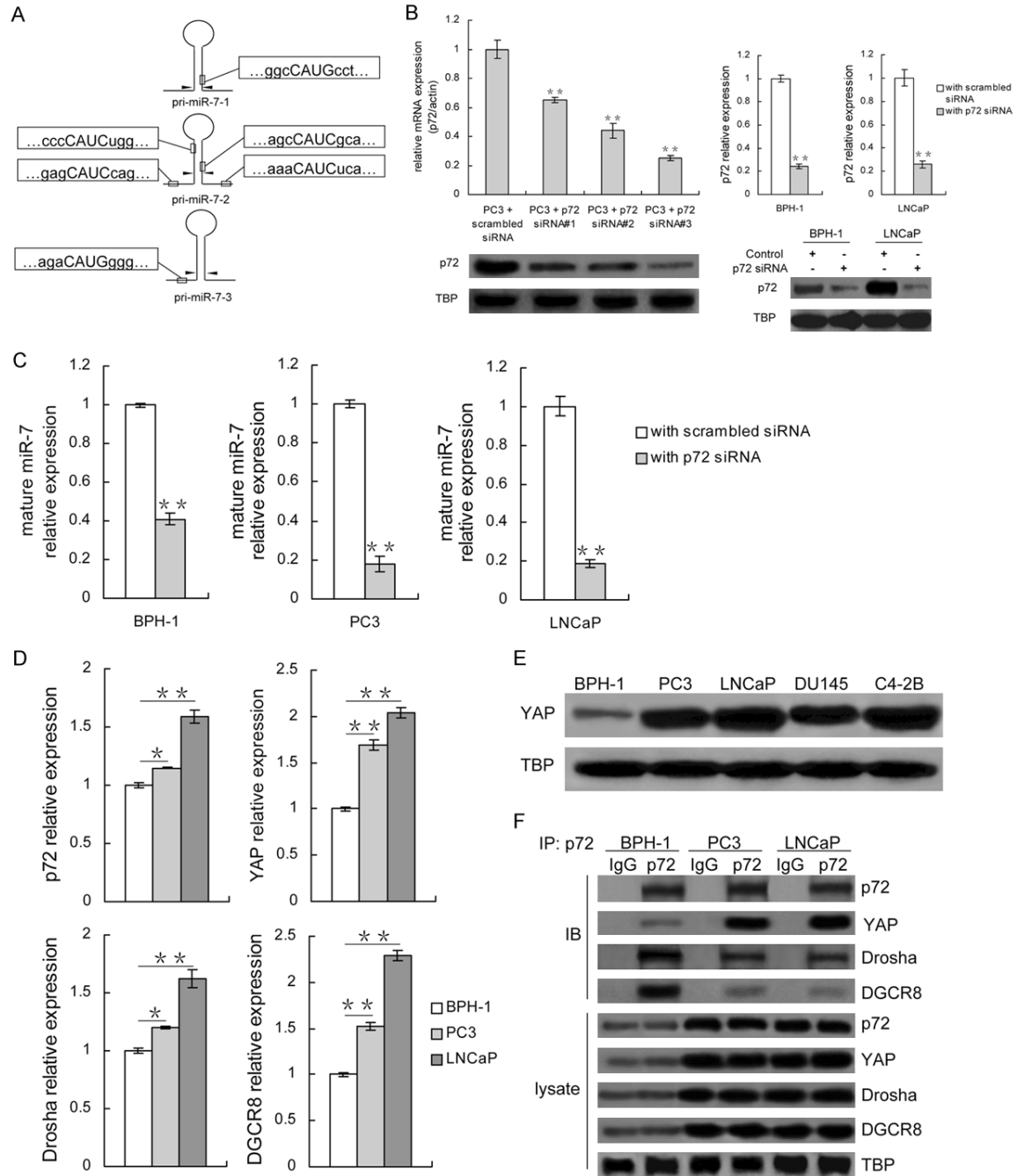


Figure 5. Processing of miR-7 primary precursors is impaired due to YAP-mediated p72 sequestration. A. Schematic of p72 binding sites (CAUC/G) on three miR-7 primary precursors. B. Expression of p72 can be inhibited by three independent siRNAs. The best effect is observed by siRNA#3. Expression of p72 is also significantly repressed in BPH-1 and LNCaP cells when using this siRNA#3. C. Expression of mature miR-7 is significantly repressed after p72 knockdown. D. Endogenous mRNA expression of p72, YAP, Drosha and DGCR8. E. Nuclear translocation of YAP is significantly enhanced in PCa cell lines. F. Endogenous interaction of p72 with YAP, Drosha and DGCR8 is identified by coIP assay. **: P<0.01; *: P<0.05.

of p72 with YAP, Drosha and DGCR8 respectively (Figure 6C). As expected, excessive interaction of YAP with p72 and attenuated p72-Dro-

sha and p72-DGCR8 interaction were observed, again indicating an impaired p72-dependent pri-miR-7s processing (Figure 6C). Col-

Imbalance of a KLF4-miR-7 loop promotes prostate cancer cell growth

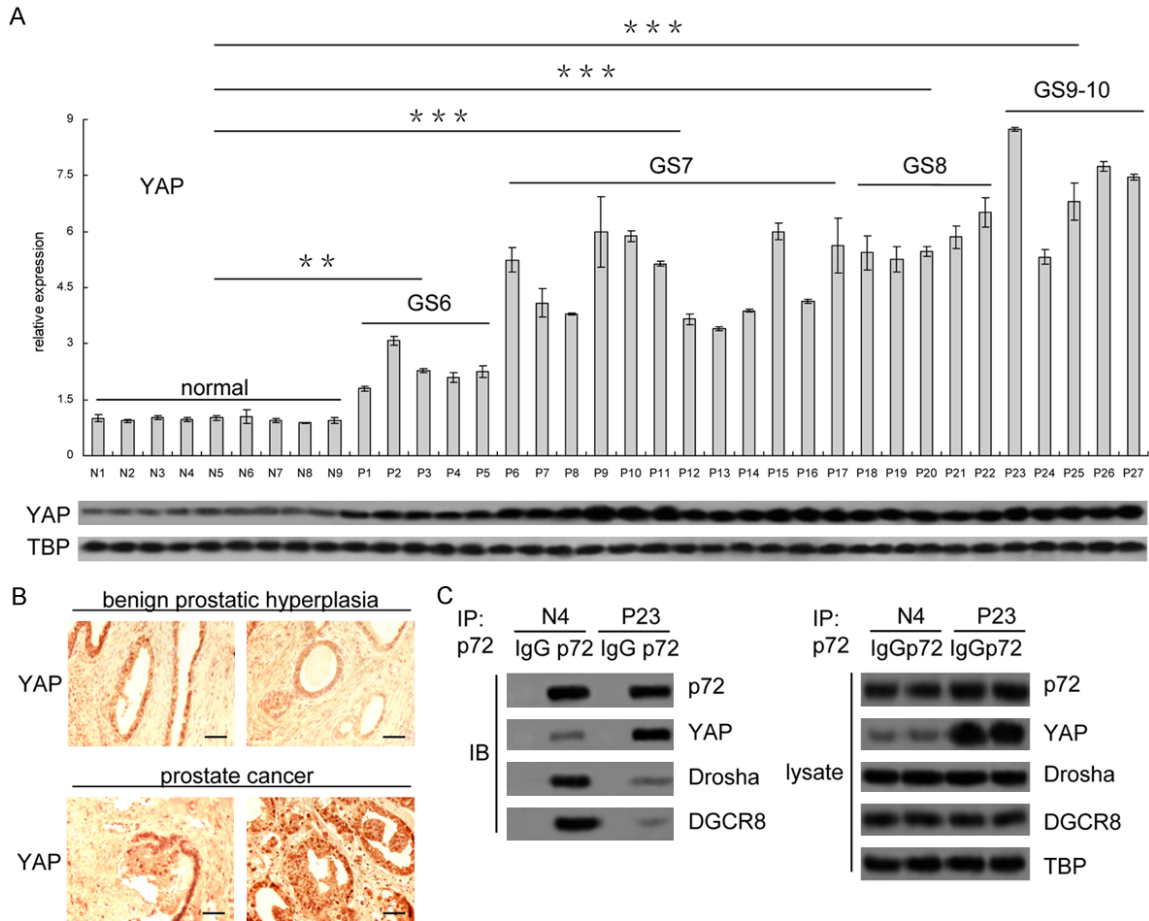


Figure 6. Expression of YAP is upregulated in clinical patient samples. **A.** Expression of YAP in both patient tumor samples (P1 to P27) and BPH samples (N1 to N9) is measured by qRT-PCR and western blot. **B.** Expression of YAP is upregulated in PCa samples by IHC staining. **C.** Interaction of p72 with YAP, Drosha and DGCR8 in both PCa and BPH samples. Scale Bar: 50 μm; ***: P<0.001; **: P<0.01.

lectively, our results indicate that dissociation of the p72/Drosha/DGCR8 complex due to YAP mediated sequestration of p72 results in the decrease in mature miR-7 production.

Pri-miR-7s processing can be restored by knockdown of YAP in PCa cells

In order to further determine that sequestration of p72 by YAP leads to a dissociation of the p72/Drosha/DGCR8 complex and a consequentially decreased production of mature miR-7 in PCa cells, we first knocked down the expression of YAP by siRNA (**Figure 7A**) and then repeated above co-IP assays to validate the interaction of p72 with Drosha and DGCR8 respectively in PCa cells. We found that YAP knockdown significantly repressed its interaction with p72 (**Figure 7B**). As a result, the inter-

action of p72 with both Drosha and DGCR8 was enhanced, indicating a restoration of the p72/Drosha/DGCR8 complex (**Figure 7B**). In addition, knockdown of YAP had no effect on the transcription of pri-miR-7s in both PC3 and LNCaP cells (**Figure 7C**) but expression of mature miR-7 was upregulated (**Figure 7D**), concomitant with a repression of KLF4 expression (**Figure 7E**), which indicate a response to the restoration of the p72/Drosha/DGCR8 complex. On the other hand, we also detected expression of Dicer, another key microprocessor for producing mature microRNAs from pre-microRNAs, in BPH-1, PC3 and LNCaP cells and found that expression of Dicer showed no significant difference in all of the three cell lines (**Figure 7F**). These data together reveal that impaired pri-miR-7s processing is mainly caused by YAP induced sequestration of p72

Imbalance of a KLF4-miR-7 loop promotes prostate cancer cell growth

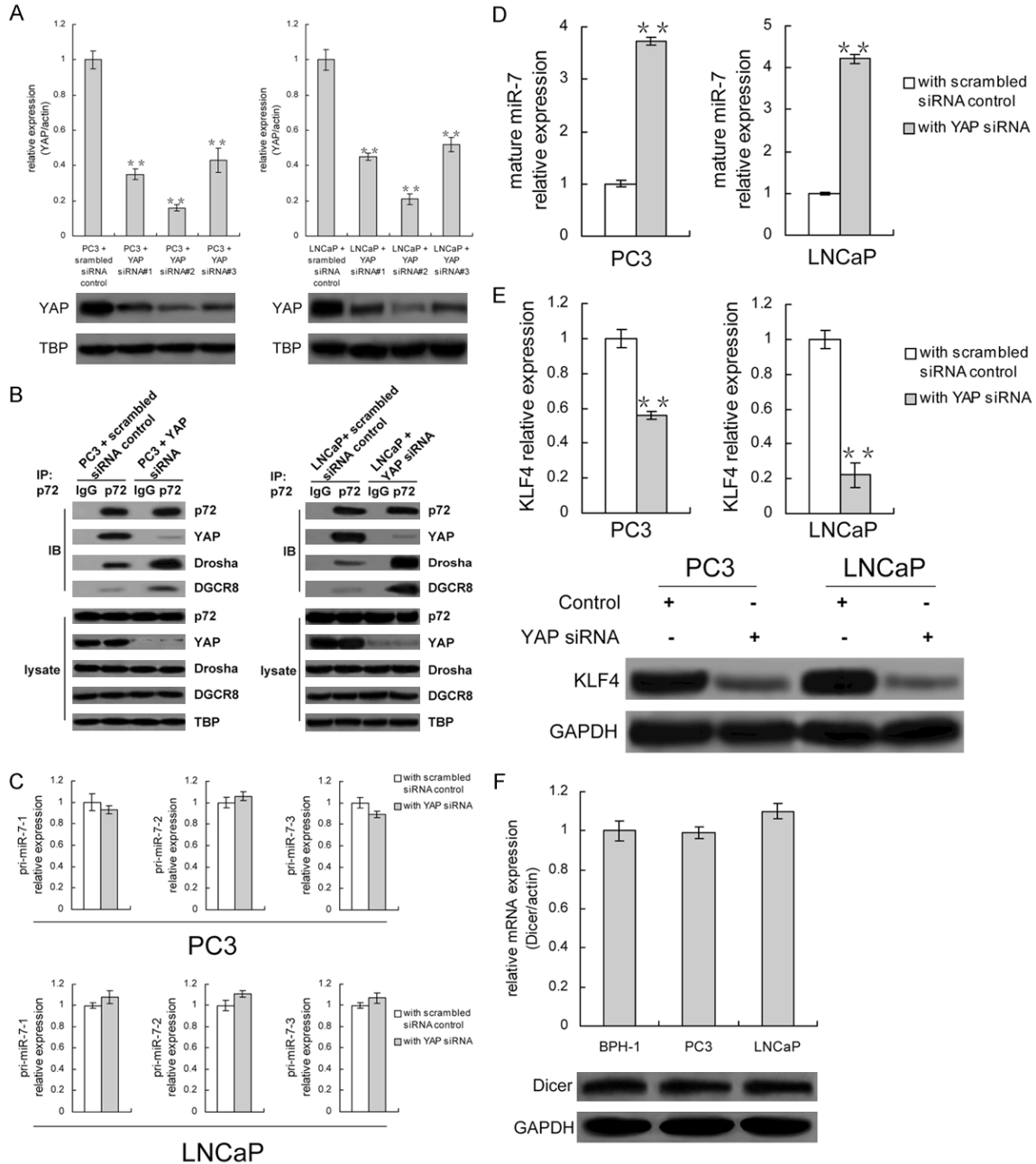


Figure 7. YAP knockdown restores mature miR-7 production. **A.** Expression of YAP can be inhibited by three independent siRNAs in both PC3 and LNCaP cells. The best effect is observed by siRNA#2 in both cell lines. **B.** YAP knockdown restores p72-Drosha and p72-DGCR8 interaction. **C.** YAP knockdown has no effect on expression of pri-miR-7s. **D.** Expression of mature miR-7 is upregulated after YAP knockdown. **E.** Expression of KLF4 is downregulated after YAP knockdown. **F.** Expression of Dicer has no difference in BPH-1, PC3 and LNCaP cells. **: P<0.01.

from the p72/Drosha/DGCR8 complex, and YAP knockdown can effectively reverse dissociation of the complex.

Overexpression of mature miR-7 mimic inhibits cell proliferation in LNCaP cells

We demonstrated in our previous work that restoration of miR-7 via ectopic stable overexpres-

sion of miR-7 primary precursors can inhibit prostatic tumor growth by specific suppression of KLF4 expression in PC3 cells [8]. So we herein wondered whether overexpression of a mature miR-7 mimic to bypass this impaired microRNA processing can also inhibit cell proliferation in LNCaP cells. For this purpose, we transiently transfected a mature miR-7 mimic

Imbalance of a KLF4-miR-7 loop promotes prostate cancer cell growth

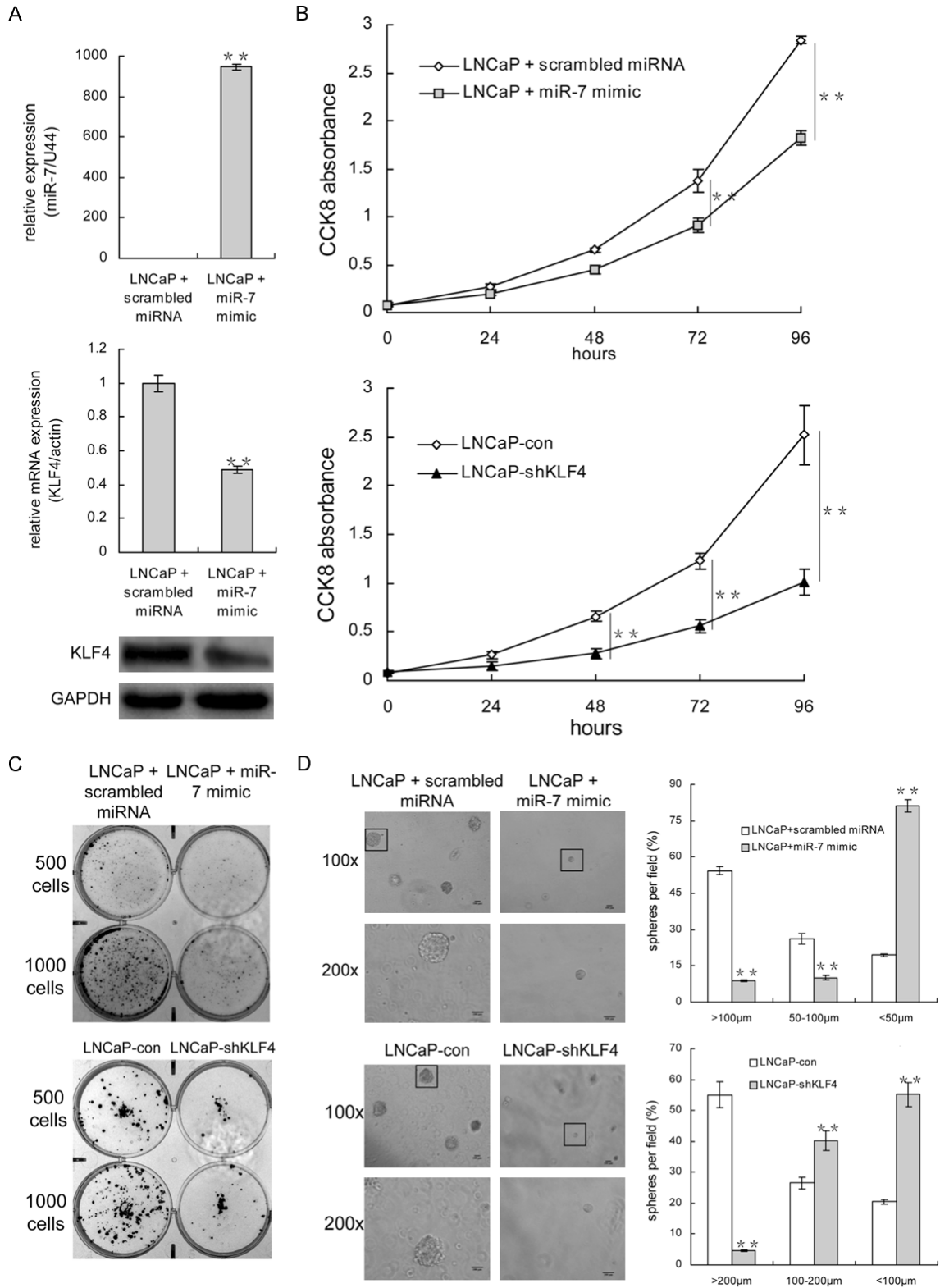


Figure 8. Overexpression of mature miR-7 mimics inhibits cell proliferation in LNCaP cells. A. Expression of mature miR-7 is upregulated and expression of KLF4 is downregulated in LNCaP cells after transfected with miR-7 mimics. B. Proliferation of LNCaP cells is detected by CCK8 assay after overexpression of mature miR-7 mimics or knockdown of KLF4. C. Proliferation of LNCaP cells is detected by 2-D plate colony formation assay after overexpression of mature miR-7 mimics or knockdown of KLF4. D. Overexpression of mature miR-7 mimics or knockdown of KLF4 inhibits 3-D sphere formation of LNCaP cells. Scale bar: 100 µm. **: P<0.01.

Imbalance of a KLF4-miR-7 loop promotes prostate cancer cell growth

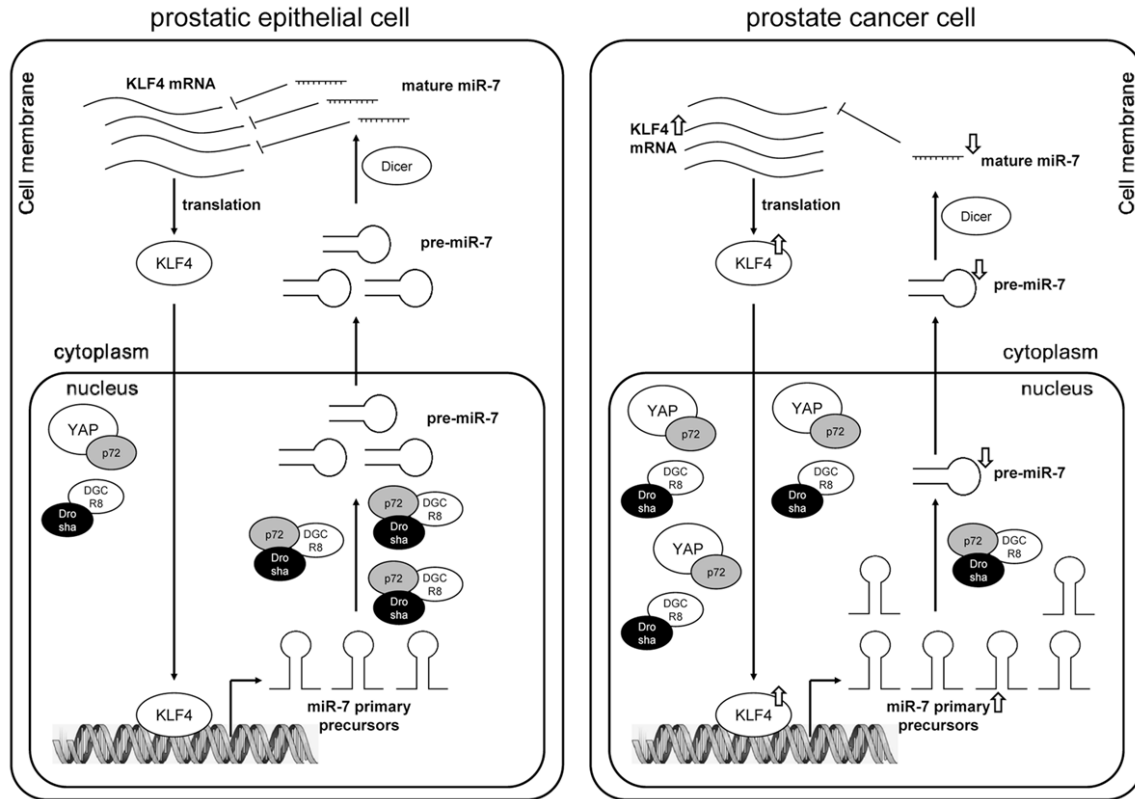


Figure 9. The KLF4-miR-7 auto-regulatory feedback loop is unbalanced in PCa cells. Enhanced nuclear translocation of oncogenic YAP sequesters p72 to dissociate the p72/Drosha/DGCR8 microprocessor complex, leading to a decreased production of mature miR-7 and an upregulation of its target KLF4. Up or down white arrow: upregulation or downregulation of gene expression.

or scrambled miRNA control in LNCaP cells and confirmed its overexpression by TaqMan microRNA assays (**Figure 8A**). We found that after miR-7 overexpression, KLF4 expression was significantly inhibited (**Figure 8A**). To evaluate possible effects of miR-7 restoration on tumor cell proliferation *in vitro*, we carried out CCK8 assay in LNCaP cells 96 hrs after transfection with a mature miR-7 mimic or the control. As shown in **Figure 8B**, the CCK8 absorbance was significantly decreased compared to the control, indicating an inhibitory effect on cell proliferation. In addition, we repeated the same assay in LNCaP-shKLF4 vs. LNCaP-con cells to verify whether restoration of miR-7 inhibits cell proliferation by directly repressing KLF4 expression. We found that CCK8 absorbance was dramatically downregulated after KLF4 knockdown (**Figure 8B**). Furthermore, in 2D plate colony formation assays, we also found that limited colonies were formed after miR-7 restoration and KLF4 knockdown presented similar results (**Figure 8C**). In 3D culture

assays, after miR-7 restoration, the cell sphere numbers with a diameter over 100 μm were significantly decreased and the diameter of over 80% cell spheres was limited to less than 50 μm (**Figure 8D**). Similarly, KLF4 knockdown dramatically downregulated the cell sphere number with large diameters (over 200 μm) and the diameter of more than 50% spheres was under 100 μm (**Figure 8D**). Taken together, all the findings demonstrate that in addition to restoration of p72-dependent pri-miR-7s processing to increase mature miR-7 production, overexpression of mature miR-7 mimic can also efficiently inhibit the proliferation of PCa cells through a direct downregulation of KLF4 expression *in vitro*.

Discussion

In this study, we demonstrated for the first time that a KLF4-miR-7 auto-regulatory feedback loop is formed to reciprocally regulate KLF4 and miR-7 expression in PCa cells (**Figure**

9). In detail, KLF4 activates the transcription of miR-7 primary precursors to produce mature miR-7 and in turn to reduce its own translation. Importantly, this feedback loop is unbalanced in PCa cell lines as well as clinical prostatic tumor samples, exhibiting an overexpression of both KLF4 and miR-7 primary precursors but a repression of mature miR-7, due to an impaired microRNA-processing. In addition, we identified p72 as a key co-factor for pri-miR-7s processing and found that nuclear translocation of oncogenic YAP is enhanced in PCa. Taken these findings together, we herein revealed that imbalance of the KLF4-miR-7 feedback loop in PCa cells is due to an attenuation of p72-dependent pri-miR-7s processing by YAP induced p72 sequestration from the p72/Drosha/DGCR8 complex, leading to a decrease of mature miR-7 production and an overexpression of KLF4 to promote PCa cell growth. Therefore, our findings suggest an unbalanced KLF4-miR-7 auto-regulatory feedback loop to activate PCa cell proliferation by repressing miR-7-induced target gene silencing.

It has been reported that KLF4 can work as an inhibitor of PCa cell growth and migration [18], and degradation of KLF4 by TGF- β can induce expression of Slug to promote EMT in PCa [19]. Interestingly, in our current study, we identified a phenotype of a subpopulation in Chinese PCa patients with elevated expression of KLF4 by qRT-PCR, western blot and IHC assay. Our finding is supported by previous works from other groups which also reported an upregulation of KLF4 in PCa tissues [20, 21] as well as by datasets from Oncomine database (**Figure 1C**). Our findings indicate that different underlying mechanisms may be involved in regulation of prostatic tumor growth with elevated expression of KLF4 compared to that with repressed KLF4 expression. In our previous work, we demonstrated that elevated expression of KLF4 plays an important role for maintaining stemness of prostate cancer stem cells to promote tumor cell growth [8]. Herein our findings give an explain for upregulation of KLF4 in PCa, that is, enhanced nuclear translocation of YAP attenuates pri-miR-7s processing to produce mature miR-7 and consequentially results in a failed repression of KLF4 expression.

A KLF4-microRNA feedback loop plays an important role in many biological processes

including maintenance of self-renewal or pluripotency of embryonic stem cells (ESC) and acceleration of somatic cell proliferation. For example, KLF4 expression can be inhibited by anti-pluripotent miR-24-3p and miR-24-2-5p as a target. In mouse ESC, KLF4 promotes the transcription of PRMT7, a new stemness-associated transcription factor, and sequentially represses the transcription of miR-24-2 gene, the primary precursor for both miR-24-3p and miR-24-2-5p, in a PRMT7-mediated manner to improve its own expression for maintenance of stemness [22]. In addition, KLF4 has also been found to accelerate proliferation of vascular smooth muscle cell (VSMC) via a miR-200c-SUMOylated KLF4 double-negative feedback loop [23]. Both KLF4 and SUMO-conjugating enzyme Ubc9 are shown to be directly inhibited by miR-200c. Moreover, KLF4 can be SUMOylated by Ubc9 to recruit transcriptional co-repressors such as NCoR and HDAC to the miR-200c promoter to repress its transcription, leading to an increased target gene (e.g. KLF4 and Ubc9) expression [23]. Besides these double-negative feedback loops, a KLF4-miR-206 auto-regulatory feedback loop has been reported to either promote or inhibit KLF4 translation depending on different cell contexts. For instance, miR-206 promotes KLF4 expression in immortalized mammary epithelial MCF10A cells opposite to its repressive function on KLF4 translation in breast cancer cell line MDA-MB-231, although KLF4 can promote the transcription of miR-206 in both two types of cells [11]. In contrast, in the present study the KLF4-miR-7 auto-regulatory feedback loop does not exhibit such cell context-dependent functional “switch”, but instead, miR-7 enables an inhibition on KLF4 expression and KLF4 promotes the transcription of miR-7 primary precursors in both BPH-1 cells and PCa cell line PC3 and LNCaP cells. The present findings add KLF4-miR-7 feedback loop as a new member to the KLF4-microRNA feedback loop list of tumor cell growth regulation.

There are several mechanisms reported to underlying the imbalance of microRNA-transcription factor feedback loops in cancer. First, mutation or deletion of microRNA binding sites in 3'- untranslated region (3'UTR) of the target gene may lead to a microRNA off-target effect [24, 25]. Second, microRNA transcription might be inactivated genetically or epigenetically [26, 27]. Third, impaired or defective microRNA-pro-

cessing, such as dysregulation of the co-factors/Drosha/DGCR8 microprocessor complex (from pri-microRNAs to pre-microRNAs) [28-30] and/or Dicer (from pre-microRNAs to mature microRNAs) [31-33], can also be another available mechanism. Results in our previous [8] and current studies reveal that restoration of miR-7 significantly inhibits KLF4 expression in PCa cells, indicating KLF4 as a miR-7 target and arguing against a microRNA off-target effect. The present KLF4 knockdown and luciferase report assay experiments make the second possibility unlikely because 1) KLF4 successfully promotes pri-miR-7s transcription; 2) No CpG islands hypermethylation is found in the promoter regions of pri-miR-7s (data not shown), indicating that pri-miR-7s transcription has no alteration. On the other hand, the current work supports the third model, that is, impaired microRNA processing appears to be the main mechanism for the imbalance of KLF4-miR-7 feedback loop. We found no significant difference at Dicer's expressional levels between BPH-1 cells and PCa cell line PC3 or LNCaP cells, but an obvious dissociation of the p72/Drosha/DGCR8 complex. Consistent with this notion, we found that enhanced nuclear translocation of oncogenic YAP sequestered p72 from the p72/Drosha/DGCR8 complex and in turn attenuated p72-dependent pri-miR-7s processing. YAP Knockdown releases p72 to re-form the p72/Drosha/DGCR8 complex. Taken together, the current study provides clear evidence that the imbalance of KLF4-miR-7 auto-regulatory feedback loop is due to a decrease of mature miR-7 production through an impaired pri-miR-7s processing.

In summary, our results point out a mutual regulatory feedback loop in which KLF4 promotes miR-7 expression while itself is downregulated by the same microRNA. In addition, we identified a novel co-activator factor p72 for pri-miR-7s processing via p72-dependent binding of pri-miR-7s for a cleavage by the canonical Drosha-DGCR8 microprocessor. However, imbalance of the feedback loop occurs in PCa cells. Mechanistically, enhanced nuclear translocation of oncogenic YAP sequesters p72 and disrupts p72-dependent pri-miR-7s processing. This YAP-induced p72 sequestration inhibits the production of mature miR-7 and impairs the inhibition of KLF4 expression, ultimately resulting in an unbalanced KLF4-miR-7 feed-

back loop in PCa cell lines as well as clinical prostatic tumor samples. Our study suggests a promising strategy for PCa therapy by YAP knockdown or by overexpression of mature miR-7 mimics to restore this auto-regulatory feedback loop.

Acknowledgements

The authors thank Dr. Fang Wang for her technical support. This work was supported by the Ministry of Science and Technology of China (2017YFA0102900), the National Natural Science Foundation of China (81301857, 81630073, 81372189), the Innovation Program of Shanghai Municipal Education Commission (14YZ035), Shanghai Jiao Tong University Foundation for Medicine-Engineering Science Project (YG2012MS47), Science and Technology Commission of Shanghai Municipality (16JC1405700) and KC Wong Foundation.

Disclosure of conflict of interest

None.

Address correspondence to: Drs. Wei-Qiang Gao and Yu-Xiang Fang, State Key Laboratory of Oncogenes and Related Genes, Renji-Med X Clinical Stem Cell Research Center, Ren Ji Hospital, School of Medicine, Shanghai Jiao Tong University, 160 Pujian Rd, Shanghai 200127, China. Tel: +86-21-6838-3917; Fax: +86-21-6838-3916; E-mail: gao.weiqiang@sjtu.edu.cn (WQG); Tel: +86-21-6838-3926; Fax: +86-21-6838-3916; E-mail: fyx2003-108@sina.com (YXF)

References

- [1] Yates LA, Norbury CJ, Gilbert RJ. The long and short of microRNA. *Cell* 2013; 153: 516-519.
- [2] Esquela-Kerscher A, Slack FJ. Oncomir-microRNAs with a role in cancer. *Nat Rev Cancer* 2006; 6: 259-269.
- [3] Zhao J, Tao Y, Zhou Y, Qin N, Chen C, Tian D, Xu L. MicroRNA-7: a promising new target in cancer therapy. *Cancer Cell Int* 2015; 15: 103.
- [4] Fang Y, Xue JL, Shen Q, Chen J, Tian L. MicroRNA-7 inhibits tumor growth and metastasis by targeting the phosphoinositide 3-kinase/Akt pathway in hepatocellular carcinoma. *Hepatology* 2012; 55: 1852-1862.
- [5] Reddy SD, Ohshiro K, Rayala SK, Kumar R. MicroRNA-7, a homeobox D10 target, inhibits p21-activated kinase 1 and regulates its functions. *Cancer Res* 2008; 68: 8195-8200.

Imbalance of a KLF4-miR-7 loop promotes prostate cancer cell growth

- [6] Zhang H, Cai K, Wang J, Wang X, Cheng K, Shi F, Jiang L, Zhang Y, Dou J. MiR-7, inhibited indirectly by lincRNA HOTAIR, directly inhibits SET-DB1 and reverses the EMT of breast cancer stem cells by downregulating the STAT3 pathway. *Stem Cells* 2014; 32: 2858-2868.
- [7] Okuda H, Xing F, Pandey PR, Sharma S, Watabe M, Pai SK, Mo YY, Iizumi-Gairani M, Hirota S, Liu Y, Wu K, Pochampally R, Watabe K. MiR-7 suppresses brain metastasis of breast cancer stem-like cells by modulating KLF4. *Cancer Res* 2013; 73: 1434-1444.
- [8] Chang YL, Zhou PJ, Wei L, Li W, Ji Z, Fang YX, Gao WQ. MicroRNA-7 inhibits the stemness of prostate cancer stem-like cells and tumorigenesis by repressing KLF4/PI3K/Akt/p21 pathway. *Oncotarget* 2015; 6: 24017-24031.
- [9] Rowland BD, Peeper DS. KLF4, p21 and context-dependent opposing forces in cancer. *Nat Rev Cancer* 2006; 6: 11-23.
- [10] Li Q, Song W, Wang W, Yao S, Tian C, Cai X, Wang L. Suppression of epithelial-mesenchymal transition in hepatocellular carcinoma cells by Kruppel-like factor 4. *Oncotarget* 2016; 7: 29749-29760.
- [11] Lin CC, Liu LZ, Addison JB, Wonderlin WF, Ivanov AV, Ruppert JM. A KLF4-miRNA-206 autoregulatory feedback loop can promote or inhibit protein translation depending upon cell context. *Mol Cell Biol* 2011; 31: 2513-2527.
- [12] Wellner U, Schubert J, Burk UC, Schmalhofer O, Zhu F, Sonntag A, Waldvogel B, Vannier C, Darling D, zur Hausen A, Brunton VG, Morton J, Sansom O, Schüler J, Stemmler MP, Herzberger C, Hopt U, Keck T, Brabletz S, Brabletz T. The EMT-activator ZEB1 promotes tumorigenicity by repressing stemness-inhibiting microRNAs. *Nat Cell Biol* 2009; 11: 1487-1495.
- [13] Ye H, Liu X, Lv M, Wu Y, Kuang S, Gong J, Yuan P, Zhong Z, Li Q, Jia H, Sun J, Chen Z, Guo AY. MicroRNA and transcription factor co-regulatory network analysis reveals miR-19 inhibits CYLD in T-cell acute lymphoblastic leukemia. *Nucleic Acids Res* 2012; 40: 5201-5214.
- [14] Busch B, Bley N, Müller S, Glaß M, Misiak D, Lederer M, Vetter M, Strauß HG, Thomssen C, Hüttelmaier S. The oncogenic triangle of HMGA2, LIN28B and IGF2BP1 antagonizes tumor-suppressive actions of the let-7 family. *Nucleic Acids Res* 2016; 44: 3845-3864.
- [15] Ma Y, Dai H, Wang L, Zhu L, Zou H, Kong X. Consent for use of clinical leftover biosample: a survey among Chinese patients and the general public. *PLoS One* 2012; 7: e36050.
- [16] Gregory RI, Yan KP, Amuthan G, Chendrimada T, Doratotaj B, Cooch N, Shiekhattar R. The Microprocessor complex mediates the genesis of microRNAs. *Nature* 2004; 432: 235-240.
- [17] Mori M, Triboulet R, Mohseni M, Schlegelmilch K, Shrestha K, Camargo FD, Gregory RI. Hippo signaling regulates microprocessor and links cell-density-dependent miRNA biogenesis to cancer. *Cell* 2014; 156: 893-906.
- [18] Wang J, Place RF, Huang V, Wang X, Noonan EJ, Magyar CE, Huang J, Li LC. Prognostic value and function of KLF4 in prostate cancer: RNAa and vector-mediated overexpression identify KLF4 as an inhibitor of tumor cell growth and migration. *Cancer Res* 2010; 70: 10182-10191.
- [19] Liu YN, Abou-Kheir W, Yin JJ, Fang L, Hynes P, Casey O, Hu D, Wan Y, Seng V, Sheppard-Tillman H, Martin P, Kelly K. Critical and reciprocal regulation of KLF4 and SLUG in transforming growth factor β -initiated prostate cancer epithelial-mesenchymal transition. *Mol Cell Biol* 2012; 32: 941-953.
- [20] Guzel E, Karatas OF, Duz MB, Solak M, Ittmann M, Ozen M. Differential expression of stem cell markers and ABCG2 in recurrent prostate cancer. *Prostate* 2014; 74: 1498-1505.
- [21] Na XY, Liu ZY, Ren PP, Yu R, Shang XS. Long non-coding RNA UCA1 contributes to the progression of prostate cancer and regulates proliferation through KLF4-KRT6/13 signaling pathway. *Int J Clin Exp Med* 2015; 8: 12609-12616.
- [22] Lee SH, Chen TY, Dhar SS, Gu B, Chen K, Kim YZ, Li W, Lee MG. A feedback loop comprising PRMT7 and miR-24-2 interplays with Oct4, Nanog, Klf4 and c-Myc to regulate stemness. *Nucleic Acids Res* 2016; 44: 10603-10618.
- [23] Zheng B, Bernier M, Zhang XH, Suzuki T, Nie CQ, Li YH, Zhang Y, Song LL, Shi HJ, Liu Y, Zheng CY, Wen JK. miR-200c-SUMOylated KLF4 feedback loop acts as a switch in transcriptional programs that control VSMC proliferation. *J Mol Cell Cardiol* 2015; 82: 201-212.
- [24] Gao Y, He Y, Ding J, Wu K, Hu B, Liu Y, Guo B, Shen Y, Landi D, Landi S, Zhou Y, Liu H. An insertion/deletion polymorphism at miRNA-122-binding site in the interleukin-1alpha 3' untranslated region confers risk for hepatocellular carcinoma. *Carcinogenesis* 2009; 30: 2064-2069.
- [25] Zhang Y, Sturgis EM, Sun Y, Sun C, Wei Q, Huang Z, Li G. A functional variant at miRNA-122 binding site in IL-1 α 3'UTR predicts risk and HPV-positive tumours of oropharyngeal cancer. *Eur J Cancer* 2015; 51: 1415-1423.
- [26] Varambally S, Cao Q, Mani RS, Shankar S, Wang X, Ateeq B, Laxman B, Cao X, Jing X, Ramnarayanan K, Brenner JC, Yu J, Kim JH, Han B, Tan P, Kumar-Sinha C, Lonigro RJ, Palanisamy N, Maher CA, Chinnaiyan AM. Genomic loss of microRNA-101 leads to overex-

Imbalance of a KLF4-miR-7 loop promotes prostate cancer cell growth

- pression of histone methyltransferase EZH2 in cancer. *Science* 2008; 322: 1695-1699.
- [27] Chu M, Chang Y, Guo Y, Wang N, Cui J, Gao WQ. Regulation and methylation of tumor suppressor miR-124 by androgen receptor in prostate cancer cells. *PLoS One* 2015; 10: e0116197.
- [28] Rupaimoole R, Wu SY, Pradeep S, Ivan C, Pecot CV, Gharpure KM, Nagaraja AS, Armaiz-Pena GN, McGuire M, Zand B, Dalton HJ, Filant J, Miller JB, Lu C, Sadaoui NC, Mangala LS, Taylor M, van den Beucken T, Koch E, Rodriguez-Aguayo C, Huang L, Bar-Eli M, Wouters BG, Radovich M, Ivan M, Calin GA, Zhang W, Lopez-Berestein G, Sood AK. Hypoxia-mediated downregulation of miRNA biogenesis promotes tumour progression. *Nat Commun* 2014; 5: 5202.
- [29] Zhu C, Chen C, Huang J, Zhang H, Zhao X, Deng R, Dou J, Jin H, Chen R, Xu M, Chen Q, Wang Y, Yu J. SUMOylation at K707 of DGCR8 controls direct function of primary microRNA. *Nucleic Acids Res* 2015; 43: 7945-7960.
- [30] Wu H, Sun S, Tu K, Gao Y, Xie B, Krainer AR, Zhu J. A splicing-independent function of SF2/ASF in microRNA processing. *Mol Cell* 2010; 38: 67-77.
- [31] Foulkes WD, Priest JR, Duchaine TF. DICER1: mutations, microRNAs and mechanisms. *Nat Rev Cancer* 2014; 14: 662-672.
- [32] van den Beucken T, Koch E, Chu K, Rupaimoole R, Prickaerts P, Adriaens M, Voncken JW, Harris AL, Buffa FM, Haider S, Starmans MHW, Yao CQ, Ivan M, Ivan C, Pecot CV, Boutros PC, Sood AK, Koritzinsky M, Wouters BG. Hypoxia promotes stem cell phenotypes and poor prognosis through epigenetic regulation of DICER. *Nat Commun* 2014; 5: 5203.
- [33] Hoffend NC, Magner WJ, Tomasi TB. The modulation of dicer regulates tumor immunogenicity in melanoma. *Oncotarget* 2016; 7: 47663-47673.